PLASMA EXPERIMENT FOR PLANETARY EXPLORATION (PEPE)

D. T. Young[1*], J. E. Nordholt[2], J. L. Burch[1], D. J. McComas[2], R.A. Abeyta[2], J. Alexander [1], J. Baldonado[2], P. Barker[2], R. K. Black[1], T. L. Booker[1], R. P. Bowman[1], P. J. Casey[1], L. Cope[2], J. P. Cravens[1], H.O. Funsten[2], R. Goldstein[1], D. R. Guerrero[1], S. F. Hahn[2], J. J. Hanley[1], B. P. Henneke[2], E. F. Horton[1], D. J. Lawrence[2], K.P. McCabe[2], R.P. Salazar[2], M. Shappirio[2], S. A. Storms[2], and C. Urdiales[1]

[1]Southwest Research Institute, San Antonio, TX
[1*]Now at: University of Michigan, Ann Arbor, MI
[2]Los Alamos National Laboratory, Los Alamos, NM
[3]Jet Propulsion Laboratory, Pasadena, CA

INTRODUCTION

Over the past few years NASA has emphasized low resource missions, spacecraft, and instruments. In 1997 the New Millennium Program (NMP) was instituted to explore and test new technologies for future flight missions. The NMP concept is to embrace technological risks that open the door to future missions while absorbing that risk in a relatively low-cost program with limited scientific objectives. Deep Space 1 (DS1) is the first of the NMP flight projects (Rayman et al, this volume; Nelson et al., this volume). The Plasma Experiment for Planetary Exploration (PEPE) was selected as one of two new technology science instruments for DS1.

Plasma instrumentation has been a part of space missions since the very beginnings of space exploration. Therefore the state of the art in instrument technology and design was already well advanced before the advent of the NMP. Although some plasma instruments can be characterized as large (roughly >10 kg), most individual instruments are in the category of a few kilograms. Mission science objectives have often been met by combining a suite of several such instruments provided by one or more investigators. It is common, for example, to have separate instruments addressing ion energy/charge (E/Q) and angular measurements, electron energy and angle measurements, and ion composition (mass/charge (M/Q)). On most spacecraft these sensors are entirely separate, for example on the Polar spacecraft (Harten and Clark, 1995). The Cassini Plasma Spectrometer (CAPS) is an example of three sensors combined into a single integrated unit (Young et al., 1998). The team from Los Alamos National Laboratory and Southwest Resarch Institute that designed and built the PEPE instrument also formed the core of the team that built the CAPS instrument.

Space flight instrumentation is generally manufactured using materials, electrical components, and manufacturing techniques that have heritage, meaning that they are well tested and largely out of date by the time the mission is operational. This conservative (and practical) approach, while successful, is unable to take advantage of the accelerated pace of aerospace and commercial technologies. The NMP, on the other hand, gives instrument designers the opportunity to incorporate cutting-edge technologies and provides a proving ground for their application. In this way NASA and the scientific

community are able to absorb and control the risk inherent in development of new technology.

Technical and Scientific Objectives

The primary objective of the NMP and of the DS1 mission is to act as a means for testing and validating new technologies that enable future missions by reducing spacecraft and instrument resources while improving performance. In addition, the DS1 mission has a number of scientific objectives that will validate the use of new instrument technologies while gathering scientific data in the solar wind, during the flyby of Asteroid Braille (1992 KD), and planned flybys of comets Wilson-Harrington and Borrelly. There are a total of twelve new technologies carried on the DS1 spacecraft, one of which is the PEPE instrument. In turn PEPE incorporates six new instrumentation technologies that are listed in Table 1. Validation of the instrument technologies requires primarily that PEPE operate according to specification and that it meet the performance and resource requirements listed respectively in Tables 2 and 3. The validation goals and performance of PEPE are discussed in detail in Young et al., 2000.

PEPE contributes to a second technology objective of the DS1 mission by making detailed measurements of the local plasma environment, thus demonstrating that similar measurements can be carried out successfully on future missions employing ion propulsion systems. The ion propulsion system will disturb the local plasma environment in a number of ways, primarily through the creation of large fluxes of backscattered ions and thermal electrons. The interaction of this plasma with the ambient solar wind is of considerable interest.

The primary scientific objective of the PEPE investigation is to study the interaction of the solar wind with small solar system bodies. On July 29, 1999 DS1 flew past Asteroid Braille (formerly 1992 KD) at a closest approach distance of 27 ± 2 km (K. Fleming, personal communication). Unfortunately the encounter miss distance was well outside the planned value of ~7 km. The encounter geometry was also outside nominal values. Those circumstances, coupled with the apparent hard mineral makeup of Braille (e.g., pyroxene or similar), limited the charged particle signal that could be expected at DS1. Indeed, the PEPE data failed to show any evidence of solar wind interaction with the asteroid.

Following the encounter with Braille, PEPE will have the opportunity to sample the comas of two very different comets in 2001. Comet Wilson Harrington is thought to be a low activity highly outgassed body with little coma activity. Although a gas outburst was observed in 1949 (Fernandez et al., 1997), it is presently unclear what the gas production rate will be during the planned encounter in early 2001. The second object, Comet Borrelly is however a relatively young object and should be relatively active. The combination of observations near these two objects will allow PEPE to break new ground in the comparative study of the evolution of cometary comas and their composition.

A second important PEPE scientific objective is the study of solar wind ion composition and ion and electron velocity distributions. DS1 and PEPE will provide a solar wind observation platform well away from the Earth during most of the mission. Data from PEPE during these periods can be applied to 3-dimensional studies of large scale structures in the solar wind, for example the evolution of coronal mass ejections from the sun. Simultaneous studies early in the DS1 mission will combine data from PEPE, Wind, ACE and Cassini plasma instruments to calibrate PEPE response. Solar wind data will also support demonstration of PEPE s operational capabilities in the plasma environment of the DS1 spacecraft. The quality, accuracy, and consistency of scientific observations of the solar wind made with PEPE will help establish the appropriateness and utility of new technologies incorporated into its design.

Instrument Overview

Figure 1 shows a photograph of the PEPE instrument. PEPE is designed to be a general-purpose plasma sensor capable of measuring electrons and mass-resolved ions over most of particle phase space from 8 eV to 33,500 eV. Because 3-axis stabilized spacecraft pose a problem for complete coverage of all possible plasma arrival directions, PEPE is also designed with a scanned field-of-view (FOV) that covers a solid angle of 2.8 π steradians once each 65 s. PEPE heritage comes largely from work at the two collaborating institutions: SwRI s development of miniaturized electrostatic analyzer optics (Young et al., 1998) and LANL s development of linear electric field (LEF) time-of flight (TOF) mass spectrographs (McComas et al., 1998; Nordholt et al., 1998). Our chief objective was to build an instrument with performance comparable to that of the Cassini Plasma Spectrometer (CAPS) on which LANL and SwRI had collaborated (together with other institutions (Young et al., 1998)), but with significantly lower resource requirements.

In order to achieve the goal of reduced resources with comparable instrument performance, elements of the CAPS electrostatic optics were either modified or entirely redesigned and miniaturized. This required the introduction of several new methods and technologies including high resistance coatings applied to the ceramic TOF cylinder, the use of metal-plated plastics in place of metallic parts, and novel optical/electronic packaging methods. In addition, the large (3.6 kg) stepper motor actuator used to rotate the entire 20 kg CAPS instrument was replaced by an electrostatically scanned FOV.

PEPE contains three sensors integrated within a single housing. CAPS, for example, incorporates seven major subsystems, including three individual sensors packaged separately. (CAPS is not alone in this respect--other charged particle investigations on Cassini and Gallileo are also made up of multi-sensor packages that meet the demands of wide-range plasma sensors for planetary missions.) PEPE incorporates two sensors and all of the other major CAPS subsystems except for the motor-actuator in a single, highly integrated package. This eliminates a significant amount of structural overhead and redundant radiation and micro-meteroid shielding as well as external cabling used to interconnect subsystems.

PEPE, like CAPS, contains a number of components such as electron multiplier detectors, carbon foils, and high ohmic surfaces that are sensitive to particulate and chemical contamination, The most sensitive CAPS instrument, the ion mass spectrometer, was protected with a cover that was deployed in flight. The two other CAPS sensors were flown without covers. Our calculations indicated that PEPE could survive the launch environment without a deployable cover, thereby saving cost, complexity and mass. Throughout ground handling, PEPE was fitted with a sealed cover through which N_2 purge gas was flushed. The cover was removed before the rocket fairing door was closed, but the purge continued through launch. PEPE in-flight performance indicates that the instrument did not suffer any deleterious effects caused by this approach.

With reference to Figure 2, the PEPE optical system is rotationally symmetric about the central vertical axis and consists entirely of electrostatic elements. The optical system consists of three main functional elements: Angular deflection optics, energy/charge analyzers, and the LEF TOF optics. PEPE is located on a bracket at the upper (+Z) end of the +X-Y panel of the spacecraft (Figure 3) such that the central plane of the PEPE FOV lies in the spacecraft XZ plane. This gives PEPE access to both the nominal solar wind direction and to the DS1 Miniaturized Camera/Spectrometer (MICAS; see paper by Soderblom et al., this volume) boresight direction located along the spacecraft +Z axis. PEPE FOV coordinates are illustrated in Figure 4. The 3-axes of the PEPE coordinate system are parallel to those of the spacecraft. Arrows in the figure indicate the sense of the numbering of angular pixels that make up the PEPE FOV. The angular coordinates for azimuth are defined between 0° and 359° and correspond to the direction of arrival for both positively and negatively charged particles (e.g., +90° azimuth indicates particles arriving from the direction of the spacecraft —Z axis). The angular coordinates for elevation (Figure 4) are defined as the direction of arrival of positively charged particles. Because of the nature of the deflection electric field that controls the PEPE elevation viewing direction, the direction of arrival of negatively charged particles is the opposite of that shown in Figure 4.

Instrument Description

Ions and electrons enter the PEPE optics through a grounded toroidal grid that defines the external acceptance aperture of the instrument. The grid also terminates the electric fields within PEPE. Immediately inside the grounded grid, ions and electrons entering PEPE experience an electric field that deflects them into the acceptance volume of the top-hat electrostatic analyzers. The deflection electric field is generated by two opposing, cylindrically symmetric toroidal electrodes. Equal voltages of opposite polarity are applied to the deflection electrodes so that, for example, ions coming from above the symmetry plane are deflected in the direction of the top-hat apertures, while electrons coming from below the plane are also deflected toward the top-hat apertures. The top-hat analyzers, one for ions and one for electrons, are positioned so that their apertures are located symmetrically above and below the central plane of the aperture. As ions and electrons enter the region of the top-hat analyzer electric fields they are deflected down or

up into their respective electrostatic energy analyzers. Up to this point the optical systems are identical for ions and electrons.

Elevation Deflection Analysis. The deflection optics consists of matching upper and lower toroidal deflectors whose shape is an exponential given by the equation:

$$z = k_1 \pm k_2 \exp[k_3(r - k_4)] \quad (1)$$

where z is the height of a point above the aperture mid-plane and r is the corresponding radius from the central axis. The value of k_4 determines the radius of the inner edge of the deflection toroids and is 6.00 cm in PEPE. Although rectilinear deflector profiles can give nearly the same performance, an exponential shape was chosen because it offers the highest deflection sensitivity for a given plate voltage (Zhigarev, 1975). The particular configuration of the deflection plates themselves was also designed to create space underneath the electrodes for the placement of high voltage supplies. This improves engineering architecture at the expense of the deflection constant and hence magnitude of the applied voltage.

The relationship between the angle of charged particle deflection (γ), the deflection voltage (V_D) in volts placed on the electrodes, and the particle energy/charge (E/Q) in eV was obtained by ray-tracing and is given by:

$$\gamma(^\circ) = k_5 \, QV_D/(E/Q) + 0.9^\circ. \quad (2)$$

Both V_D and Q are to be taken as signed quantities. Thus, for electrons Q = -1 and if V_D is positive then γ is a negative quantity in Figure 4. The nominal value of $k_5 = 134.5^\circ$ per charge with a slight variation of < 1% over the elevation range of $\pm 45^\circ$. The constant of 0.9° represents an offset in the top-hat field of view. Voltages up to a maximum of $\pm$ 5000 V can be applied to the electrodes which places a limiting value on the maximum angle through which particles of a given energy can be deflected:

$$\gamma_{max}(^\circ) = 6.725 \times 10^5/(E/Q). \quad (3)$$

This means that the maximum FOV deflection at the upper limit of the PEPE energy range (33,500 eV) is 20.0° per charge. The angular resolution of the instantaneous FOV is 4° FWHM for electrons and 3.6° FWHM for ions. These values are set by the separation of the deflection electrodes and the intervening collimation (Figure 2) and ar designed to match the acceptance aperture of the ESA optics.

Different angular directions are accepted by stepping the deflection voltages through a program that causes the central FOV angle of regard to move from - 45° to + 45° (or vice versa depending on charge sign) in 16 linearly spaced steps. Equation (2) shows the relationship between particle energy/charge and the deflection angle. This

implies that the voltage V_D is dependent on the voltage V_E that is applied to the energy/charge analyzer and determines the energy of particles accepted.

(5)

Energy/charge and Angle. After passing through the angle deflection electrodes, ions and electrons enter an electric field created by two facing toroidal top-hat ESA s. Each ESA consists of concentric toroidal electrodes with a cutout in the outer electrode which functions as the ESA entrance aperture. Toroidal shapes are chosen because they result in a larger aperture area per unit of ESA electrode area (Young et al.,1989). When a voltage is applied to the inner electrode (positive for the electron ESA, negative for the ion ESA), charged particles with the appropriate energy/charge and angle travel through the electric field to the exit of the ESA. Different energies are sampled by stepping the voltage on the ESA inner toroids. At the same time that the ESA voltage is stepped, so is the deflection voltage according to the relation given by (5).

The open area formed by cutouts in the outer, grounded ESA toroids expose the oppositely charged inner toroids. This sets up an electric field that deflects ions and electrons into their respective energy analyzers. The toroidal apertures are set back 15° from the vertical. The ESAs are designed so that electrons travel through a bending angle of 90°, 75° of which are spent in the ESA. Ions travel through a total bending angle of 115° of which 100° are in the ESA. The combination of toroidal electrode separation and ESA bending angle sets the energy passband at $\Delta E/E = 0.085$ (FWHM) for the electron ESA and 0.050 for the ion ESA.

The relationship of voltage on the ESA to ion and electron E/Q is given by:

$$E/Q = k_6 V_E \qquad (4)$$

Where $k_6 = 13.07$ is an unsigned constant of the ESA geometry and is identical for the ion and electron analyzers. Substitution of Equation (4) into (2) gives the control equation for the combined deflection/energy analyzer system:

$$\gamma(^\circ) = 10.27\ V_D/V_E. \qquad (5)$$

Electrons exiting the electron ESA are accelerated by + 200 V onto a conversion dynode. Electric fields in the dynode/MCP volume focus the electrons in two directions so that beam image size is kept to a minimum and azimuthal angle of arrival information is preserved. The purpose of the dynode optics is to convert incoming primary electrons into secondary electrons of a few eV that can be easily focused on to a 25 mm active diameter MCP. The toroid major radius at which the electrons exit the ESA is 41.66 mm, whereas the area onto which they are focused on the MCP is an annulus 6 to 12 mm in radius. The chief considerations in using the conversion dynode were reduction in the volume and complexity of a larger diameter MCP and holder, and reduction in overall detector background. The secondary electron yield of the nickel-plated Noryl™ plastic dynode material for penetrating energetic electrons is low relative to the efficiency of

MCP s for these particles. The relative background improvement is calculated to be a factor of ~3 (Young et al., 1998).

The electron detector consists of a stack of 3 individual MCP s arranged in Z-configuration. The MCP is operated with the entrance plate near ground potential and the exit at up to +3600V. Large (~ 0.5 cm^3) high voltage capacitors are needed to couple MCP pulses to signal amplifiers whose inputs are near ground. The azimuthal FOV is divided into 16 sectors that require 16 anodes and corresponding signal chains and coupling capacitors. In order to save volume, the printed circuit board itself (made of Rogers Corp. TMM3™) was incorporated as the capacitor dielectric material sandwiched between the 16 anodes and the corresponding Amptec A111 amplifier inputs.

The ion ESA bending angle of 100° was chosen to match the conical shape of the top of the LEF time-of-flight cylinder to which it is interfaced. Ions that exit the ESA are accelerated by voltages between —8 kV and —15 kV onto ultra-thin (nominally 0.5~1.0 $\mu g/cm^2$) carbon foils located at the entrance to the LEF TOF analyzer. (Although PEPE can operate at acceleration voltages below —15kV, the latter is the nominal operating potential and will be used as the standard value throughout the paper.) A slit electrode biased at 50% of the ESA inner toroid voltage is located 1.5 mm past the ESA exit. This electrode prevents fringing fields created by the —15 kV acceleration potential from penetrating back into the ESA and causing unwanted trajectory deflections. A uniform electric field inside the acceleration region leading up to the carbon foils is ensured by the use of a high resistance coating on the inside wall of the ceramic cylinder in the portion of the TOF section above the —15kV electrode (see discussion below).

LEF TOF Analyzer. Ions enter the LEF TOF analyzer after being accelerated by up to —15kV. Acceleration by 15kV ensures that even the lowest energy ions will pass through the carbon foils with high probability and relatively small scattering angles. When (positive) ions pass through the carbon foils their charge state may be changed. Usually this means that the ion will attach an electron upon exiting the foil and will be neutralized as a result. A relatively small percentage of ions (usually a few percent to ~30% depending on species and incident energy) will exit the foil positively charged. Furthermore, a varying percentage (from a few to ~ 30% depending on energy and species) of incident ion species with finite electron affinities (primarily H, C, and O) will exit the foils in a negative charge state (Burgi et al., 1990; Funsten et al. 1993).

The LEF TOF mass analyzer processes neutralized and charged ions differently. In the case of neutralized ions, time-of-flight analysis of neutralized ions is performed in the following manner: Ions exiting the carbon foil eject one or more secondary electrons. These are focused and accelerated into an annular outer (start) section of the MCP located at the far end of the time-of-flight section (Figure 5). When the electrons are detected in the outer portion of the MCP, a signal is sent to the PEPE time-to-digital converter to start a 83 MHz clock. The LEF optics are designed so that the neutralized ion reaches the center portion of the micro-channel plate. When detected by the MCP, the time-to-digital converter clock is stopped, a vernier is applied to the time measurement, and the time of arrival as well as the information that the center (stop) section of the

MCP was struck is recorded. Because energy per charge of the ion, the length of the time-of-flight section, and the time-of-flight is now known, the mass per charge of the ion can in principle be deduced from the following equation:

$$M/Q=2(E/Q - E_{loss}/Q + V_{acc})(T/D)^2 \quad (6)$$

Where M is the mass of the incoming ion with energy/charge E/Q exiting the ESA, E_{loss} is the amount of energy lost due to ion scattering in the foil, V_{acc} is the TOF acceleration voltage, D is the average length of the time-of-flight section and T is the time-of-flight. This is called straight through or linear mass analysis because the electric fields inside the mass-analysis section do not affect particles neutralized in the foils. The mass resolution of this type of analysis is typically low, primarily because of variations in path length and particle energy introduced by the ESA, TOF geometry (finite foil and MCP stop region sizes), and scattering in the foil. Both the foil and the MCP have finite dimensions and the geometric paths of neutrals through the TOF analyzer are not constrained. Therefore a relatively large range of path lengths is possible. Which path is taken depends on the entry point of the ion on the foil and on the angle through which individual neutrals are scattered in the foil. Secondly, the energy of ions striking the foils varies within a range of 5% set by ESA resolution. Furthermore, during traversal of the foils energy variations are introduced by scattering. Lastly, the finite resolution of the time-to-digital converter introduces relatively small errors. Thus the finite size of the LEF TOF optical elements (ESA exit aperture, foil and MCP) and the random scattering in angle and energy introduce a number of uncertainties into the TOF measurement. The resulting theoretical mass per charge resolution can be expressed by adding the RMS values of these quantities (Betts, 1979):

$$\Delta(M/Q)/(M/Q) = \{\Sigma_{\Delta E}[\Delta E/(E/Q - E_{loss}/Q + V_{acc})]^2 + [2\Delta D/D]^2 + [2\Delta T/T]^2\}^{1/2}. \quad (7)$$

Where ΔE represents each uncertainty in energy introduced by resolution and energy scattering effects, the sum ($\Sigma_{\Delta E}$) is over all such energy terms, E is the total particle energy entering the foil, $\Delta D/D$ represents path length variations, and $\Delta T/T$ is the electronic timing uncertainty.

In the case where the ions emerge from the carbon foil with a charge state other than zero, they will be deflected by the electric field induced in the TOF section. This electric field is produced by a —15kV potential applied to the entrance to the TOF section and a matching +15kV potential applied to a spherical-shaped grid at the exit of the region. The potentials create a well-defined voltage drop of 30 kV along the sides of the TOF section induced by a resistive coating. The coating is applied to different sections of the time-of-flight region with different methods. Deposition of a constant thickness coating produced a constant drop in voltage. Deposition of a varying thickness that decreases proportionally to the distance from the foils squared produces a comparable variation in the voltage distribution and a linearly increasing electric field with distance from the foils. This carefully constructed electric field creates a restoring force on the ions in the direction of the axis asymmetry. The force varies linearly along the axis of symmetry and

is pointed towards the entrance (carbon foil) end of the TOF section. Ion trajectories are confined to the center of the TOF cylinder so that the linear electric field is not disturbed by any slight variations or irregularities in the coatings. Ions below an energy of approximately 18 keV will bounce in the field, executing simple harmonic motion as they do so (Figure 5). As a consequence, ion energy and flight path in the LEF portion of the TOF do not affect flight times with the result that mass resolution is increased over that of the straight through paths described above. The ions act as though they were a simple mass on a spring and thus the time of an oscillation in the linear electric field region is proportional only to the mass per charge of the particle. (McComas and Nordholt, 1990). Ions with energies above ≈ 18 keV will exit the LEF without undergoing a bouncing motion. Similarly, ions that leave the foil negatively charged will be accelerated by the LEF down on to the stop region of the MCP and analyzed with intermediate mass resolution.

At the end of their oscillation nearly 100% of the ions strike a secondary emitter located at the center of the foil-end of the time-of-flight cylinder. Because of the properties of the cylindrical electric field, ions that do not pass close to the center of the LEF are deflected towards the cylinder walls and do not contribute to the signal. Electrons ejected by the secondary emitter are focused onto the stop region of the MCP and are processed in exactly the same manner as the straight-through events described above. Because the energy, angle, and variable path to length are no longer in the equation for mass per charge of particle, mass resolution improves to $M/\Delta M \approx 20$.

LEF TOF Electronics. The MCP housing for the time-of-flight section is also a new design. A chevron configuration of two high-gain MCPs is used instead of a standard z-stack of three MCPs. The MCP holder is highly integrated and fits directly into the bottom of the time-of-flight stack. The capacitors and resistor needed to bias the MCP stack and decouple signals are built directly into the MCP holder (Figure 6). The anode is integrated behind the MCP holder and pins from it couple directly into the amplifier and discriminator electronics (termed the front-end electronics (FEE)) board. The result is an extremely rugged, compact, and lightweight design.

All time-of-flight information is processed on the FEE board via high-speed discriminators that encode the start channel that was hit as well as initiating the time-to-digital (TDC) clock. In PEPE, three constant fraction discriminators are coupled together to read out 8 individual anodes in a coded form. Each amplifier/discriminator is built as a chip-on-board (COB) module and 2 sets of 3 each are used to read out a total of 16 anodes. Eight of the anodes are devoted to coarse measurement sectors, 6 that cover 41¡ each and 2 that cover 20.5¡ each. Eight fine sector anodes cover 5.125¡ each. The symmetry of the PEPE entrance optics requires that all anodes have a boundary at least every 45¡ (Figure 7). Anode information is used to determine from which azimuthal sector of the sky the ion entered. The voltage settings for the elevation and energy analyzers are also reported so that all of the energy and angular information for a given particle is known before any time-of-flight measurement is made. All signals from the start anodes are recorded as ion singles data. The angular mapping of the PEPE field of view as seen from PEPE s position on the spacecraft can be seen by combining the

look angles in Figure 6 with the coordinate definitions given in Figure 4. The sense of the coordinate system is the same in both figures.

The central section of the stop MCP has its own high-speed discriminator which, when triggered, stops the TDC clock. Each amplifier/discriminator consumes only 35mW with transition times <1ns. The amplifier/discriminators use balanced input differential voltages and have a 25,000 electron ($25ke^-$) RMS equivalent noise with a $150ke^-$ threshold level (equivalent to 75mV). A minimum signal of $300ke^-$ is required from the MCP to achieve <1ns timing error.

The TDC is similar to that used in the Cassini CAPS ion mass spectrometer (IMS). To save power, the base oscillator runs at only 83 MHz. The timing resolution of 750 ps is achieved by routing the start and stop signals into a vernier delay line which determines the ion time-of-flight to full resolution. Bin widths may vary as much as 100ps in a repeating pattern because of variations in the width of the taps in the delay line. The TDC range is 40ns to 1536ns with a pulse-pair resolution of 40ns. The dead-time of the TOF read-out and sorting electronics is 1.74μs. Singles data, on the other hand, are recorded with a dead time of 150 ns. The TDC includes its own built-in test (BIT) that allows all of the COBs to be tested by injecting a charge pulse at their inputs. A variable start-to-stop delay is also incorporated so that timing measurements can be checked. This makes it possible to test the entire signal chain from the anode to the DPU with the BIT. Correct operation can be verified at integration time or in flight. The TDC/FEE system also has its own ground support equipment (GSE) and simulator so that the TDC/FEE/TOF ion analysis section can be tested independently of the DPU and the DPU can be run with known inputs from a TDC simulator.

The entire PEPE ion mass analysis system weighs less than 1 kg, uses less than one watt of power, is extremely compact and is designed to be integrated very tightly with the power supplies that drive it. Close integration with the power supplies is important to keep the mass and volume of PEPE down. Often, TOF mass spectrometers using high voltages require large standoff distances that translate into a large volume and thus a high mass device. The 15kV and ion MCP high voltage power supplies are designed to plug directly into the time-of-flight cylinder without the use of conventional high voltage connectors or cables.

High Voltage Power Supply Subsystem. The PEPE electrostatic optics and MCP detectors nominally require 8 high voltage sources ranging in maximum absolute values from 3600 V for the MCPs to 15,000 V for the TOF (see the system block diagram, Figure 8). Four of these voltages (two for MCPs and positive and negative 15,000 V for the LEF TOF) are obtained from independently programmable high voltage power supplies (HVPS) that are adjustable over an 8-bit range but are otherwise static. Each deflection electrode requires a programmable bi-polar stepping supply (i.e., one that simultaneously creates equal negative and positive potentials) while the ion and electron ESA s are operated from two independent supplies. The most efficient way to generate the interrelated deflection and ESA voltages is to employ a so-called bulk supply that biases the two bi-polar deflection supplies and the ESA supplies into a coarse operating

range from which finer voltage steps can be set (Figure 8). The result is a power and component efficient system with 12-bit programmable high voltage control between ± 2500 V for the ESA s and ± 5000 V for the deflection electrodes.

Because of the large number of HVPS in PEPE, efficient packaging of the supplies was critical. The method chosen eliminated HV cables and bulky connectors entirely. As mentioned above, the ion MCP and the two TOF supplies are each built into small easily installed metal-plated plastic boxes that insert into the central portion of the PEPE body. High voltage connectors are standard pin and socket connectors with insulating sleeves that interleave as the pins mate. The electron MCP supply is located on the same circuit board as the MCP and amplifiers. Because of the need for close proximity of supplies to the deflection and ESA electrodes, each ESA supply is located on a single circuit board that also carries the inner ESA toroid, inside of which is the ESA supply. The bi-polar deflection supplies are imbedded within the structure that supports the deflection electrodes (Figure 2). The interiors of all HVPS housings were parylene coated to passivate high voltage components and increase the dielectric strength of the housing insulation.

Instrument Operation. Energy/angle scan programs are controlled by re-programmable voltage tables stored in on-board memory. The ESA voltage is held constant at one of 120 levels while the deflection voltage is stepped over a program of 16 linearly-spaced voltages that follow Equation 5. Each step is held for 32 ms so that a full elevation scan of ±45° is covered in 512 ms. Out of the 32.0 ms interval, 4.0 ms is set aside as settling time for the high voltage supplies. After a deflection voltage sweep is completed, the ESA voltage is advanced to the next step. ESA steps are spaced at logarithmic intervals such that the energy range is covered in 120 contiguous steps. Eight additional steps, during which the ESA is held at zero voltage, are used for detector background measurements. The complete elevation angle/energy range of PEPE is covered in 16 x 128 x 0.032 s = 65.536 s. In order to enhance PEPE performance during the flyby of Asteroid Braille, a fast-scanning mode was created that covered a smaller region of interest (ROI) in energy/angle space (16 deflection x 16 energy steps) using a shorter sampling interval of 8.0 ms.

Data Acquisition and Handling Subsystem. During each 32.0 ms sample interval, data from the 16 angle-sorted electron and ion counter/registers as well as valid ion TOF event and related logical event registers are accumulated in a double-buffered dual-ported memory in the data acquisition subsystem (DAQ) (Figure 8). Data continue to be accumulated throughout one full angle/energy scan (65.5 s) at the end of which they are made available to the Harris RTX2010 microprocessor. The ion and electron data are stored in the MQ, TOF, and SINGLES memories that are operated in ping-pong fashion in order to allow the processor to move and operate on the previous cycle s data while new data are being acquired. An entire cycle of science data, including housekeeping and status information, is stored in processor resident memory to permit compression prior to formatting into CCSDS packets for transmission to the spacecraft data handling system.

The PEPE data array contains a total of about 2.1 Mbytes of data acquired over 65.5 s. These data are transmitted to the ground at a maximum rate of 1024 bits/s thus requiring a compression ratio of roughly 32:1. Compression is achieved primarily by summing over 4 adjacent elevation and azimuthal angular channels and over two adjacent energy channels, thus reducing the angle/energy array from 16 x 16 x 120 elements to 4 x 4 x 60 elements. The TOF array is also summed over 4 adjacent channels. This compression scheme can be re-programmed in many ways in order to place the emphasis of the transmitted data on specific regions of interest within the data array. A second option for controlling the transmitted data products is to reprogram the angle/energy voltage scan table, creating a special region of interest (ROI) within the scan space of the instrument. Summing over these data then produces a higher resolution energy/angle scan that is averaged over the same 65.5 s time interval. This option was used for observations during the close-approach section of the asteroid flyby. Still a third option is to transmit the entire uncompressed data matrix over a period of 32 x 65.5 s = 35 minutes.

Initial Operations and Results

PEPE became fully operational on December 9, 1998. With a few minor exceptions it has operated nominally since that date. Figure 9 shows electron and ion energy spectra characteristic of PEPE s response to the local DS1 plasma environment. The vertical axis corresponds to counts/0.892 s (each data point represents a sum over 32 samples comprising 4 elevation x 4 azimuth x 2 energy individual samples). The horizontal axis is energy in eV (the graphs are plotted with highest energies at the right). The first 4 data points to the left in each spectrum are the (summed) background channels demonstrating low background rates of ~ 1 count/cm^2 as expected for MCP detectors. Both ion and electron spectra start at 8.0 eV. The slight peak in low energy electrons is due to photoelectrons from the DS1 spacecraft. The rates in this part of the spectrum typically vary by a factor of 5 with azimuthal viewing angle, indicating an irregular distribution of photoelectrons around the spacecraft. There is a broad peak in the electron distribution centered at about 30 eV, corresponding to the maximum in the solar wind electron distribution that tails off at about 1.0 keV. Initial analysis of the spectra indicates that the shape of the solar wind electron distribution is sharper than expected for a maxwellian distribution drifting at the solar wind velocity. One interpretation of the apparent excess of electrons near the peak of the distribution is that they originate in spacecraft photoelectrons that are accelerated locally by differential charging on the DS1 spacecraft caused, e. g., by the solar arrays. The rise in electron flux at energies above ~ 2 keV is an artifact of the sensor that is not well understood but is in some way related to spacecraft attitude.

The corresponding ion spectra show a peak in counts at the expected location of the solar wind H^+ ion peak flux. In this case a secondary peak attributable to He^{2+} ions is readily evident. The location of these two peaks in elevation and azimuthal angular channels agrees with the expected location of the solar wind beam in relation to the spacecraft attitude. Figure 10 shows an ion TOF spectrum obtained using a direct-events mode of the TDC that permits recording TOF events at the maximum resolution possible. Peaks caused by solar wind H^+, He^{2+}, and high charge state ions are clearly evident in the

spectrum. (It should be noted that the PEPE LEF TOF analyzer is not designed to separate low M/Q-value solar wind ions but rather higher mass singly-charged ions characteristic of cometary plasma.)

Figure 11 shows typical PEPE solar wind data taken during the period from 0000 to 0600 UT on Feb. 19, 1999. Data are displayed in an energy-time spectrogram format and were obtained during a period when the PEPE data rate was a maximum of 1024 bits/s. The ion data (Figure 11a) show an abrupt change in solar wind flux and composition at approximately 0113 UT. Electrons (Figure 11b) are also more intense at this time following a drop in the mean electron energy and a possible shift in the spacecraft potential as well. Figure 11c shows a spectrogram of PEPE TOF spectra summed over energy displayed for the same 6-hour period.

Figure 12 shows a similar set of PEPE data from the period 0000 to 0600 UT on April 27, 1999. From 0000 to 0342 UT PEPE was in its 100 bit/s telemetry mode. The data gap occurs as the PEPE data mode is changed to 1024 bits/s and the energy threshold of the PEPE ESA scan is increased from 8 to 16 eV in order to avoid the intense low energy plasma fluxes caused by the operation of the DS1 Ion Propulsion System (IPS). This transition is followed at by an increase in electron fluxes between 16 and ~50 eV and >3500 eV centered on 0410 UT and apparently related to the release of xenon gas prior to the startup of the IPS plasma source. The large flux of neutral xenon gas should give rise to a large number of photoelectrons, but the cause of the increase in keV-energy electrons is not known at this time. Electron and ion fluxes increase abruptly at 0425 UT, corresponding to the start-up of the IPS Xe+ beam. The response of the PEPE instrument to Xe+ ions has been examined by Wang et al., 1999. The data in Figure 12 clearly demonstrate that while solar wind ion observations can be made during IPS operations, electron observations are problematic due to the overwhelming flux of low-energy electrons escaping from the IPS neutralizer (see paper by Brinza et al., this volume).

Summary and Conclusions

The PEPE investigation has demonstrated that low energy plasma measurements can be made from spacecraft powered by ion propulsion systems. We have not recorded any long-term effects from the IPS ion beam that prevent operation of plasma instruments during the cruise phase of such missions. At the same time, we have shown that while solar wind ion measurements may be made simultaneously with the operation of the IPS beam, low energy (< 50 eV) electron and ions measurements are problematic.

Development of the PEPE instrument has shown that new technologies can be used to save substantially on resources required to make comprehensive space plasma measurements. It also demonstrates that the reduced-resource instruments such as PEPE can still provide high quality plasma science data. The innovative technologies used to develop PEPE can be applied with confidence to other instruments. The PEPE optical design has proven effective and can be applied regardless of the technologies used to other magnetospheric missions, planetary and otherwise. While validation of the PEPE is essentially complete, scientific analysis of data needed for final verification of PEPE performance is only beginning.

Tables

Table 1. PEPE New Technologies

1.	Miniaturized Linear Electric Field Time-of-Flight mass spectrograph
2.	Comprehensive integrated ion/electron optics
3.	Low resource, high performance data acquisition system
4.	Low resource high voltage power supplies operating up to 15,000 V
5.	Low resource high speed digital TOF electronics with 0.75ns resolution
6.	High density electro-optical packaging

Table 2. PEPE Performance Summary

Parameter	Range/Resolution	Performance	Units
Energy	Range	8.0 to 33,500	eV/e
	Range scan	120 steps, log-spaced	
	Resolution (electrons)	0.085	ΔE/E
	Resolution (ions)	0.046	ΔE/E
	Analyzer constant	13.07	
Mass	Range	1 to 135	amu/e
	Resolution (straight thru)	~4	M/ΔM
	Resolution (LEF)	~20	M/ΔM
Angle	Range (EL)	- 45° to + 45°	
	Range scan (EL)	16 steps, linear	
	EL deflection constant	$6.7 \times 10^5/(E/Q)$	(°/V)
	Range (AZ)	360°	
	Solid angle coverage	8.9	sr
	Resolution (electrons, EL x AZ)	256 pix @5° x 22°	
	Resolution (ions, EL x AZ)	128 pix @ 5° x 5°	
	Resolution (ions, EL x AZ)	32 pix @ 5° x 22°	
	Resolution (ions, EL x AZ)	96 pix @ 5° x 45°	
Temporal	AZ x TOF	0.008/0.032	s
	AZ x EL x TOF	0.128/0.512	s
	AZ x EL x EN x TOF	16.38/65.536	s
Sensitivity*	Electrons (5° x 22° pixel)	1.5×10^{-4}	cm^2 sr
	Ions (5° x 22° pixel)	8×10^{-5}	cm^2 sr
	Ions (5° x 22° pix. TOF @ ±8kV)	3×10^{-5}	cm^2 sr

*Estimated based on ray-tracing.

Table 3. PEPE Resources

Parameter	Resource	Units
Mass	5.5	kg
Power (average)	9.6	W
Volume	7.25	liters
Density	0.83	g/cm^3
Telemetry (commandable	1024, 512, 250, 100, 50, 25	bits/s
Operating range	-20 to +35	C

Figures and Captions

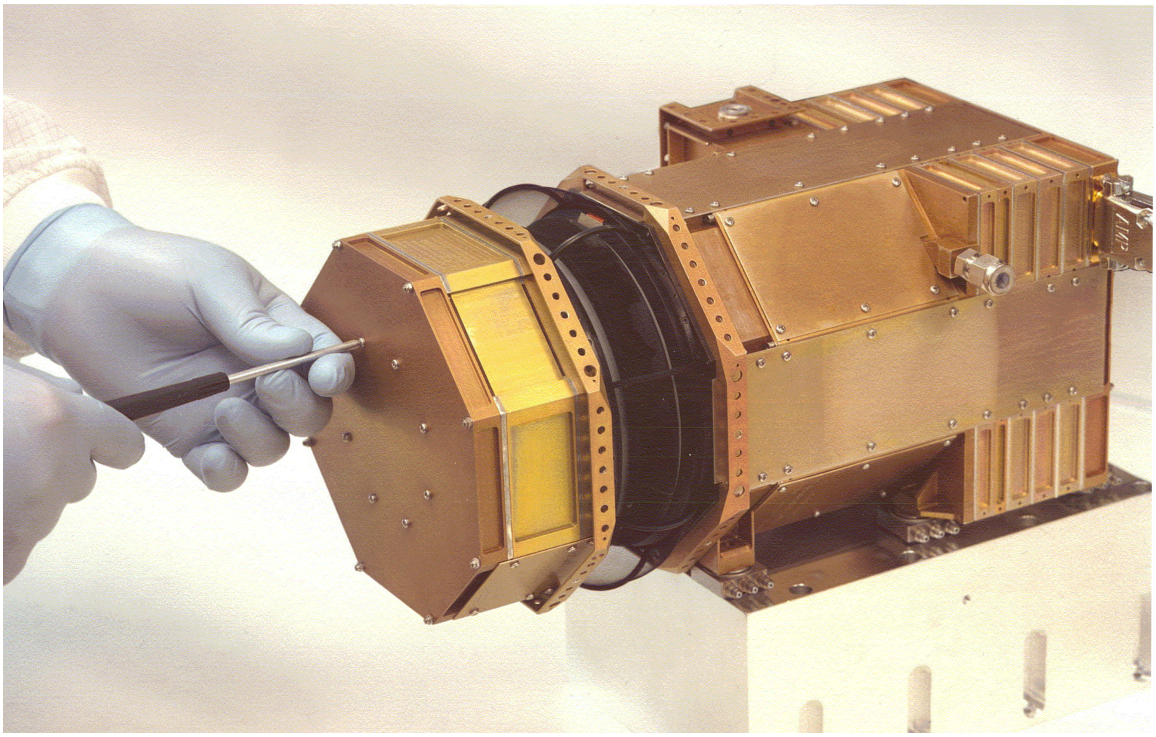

Figure 1. Photograph of the PEPE instrument.

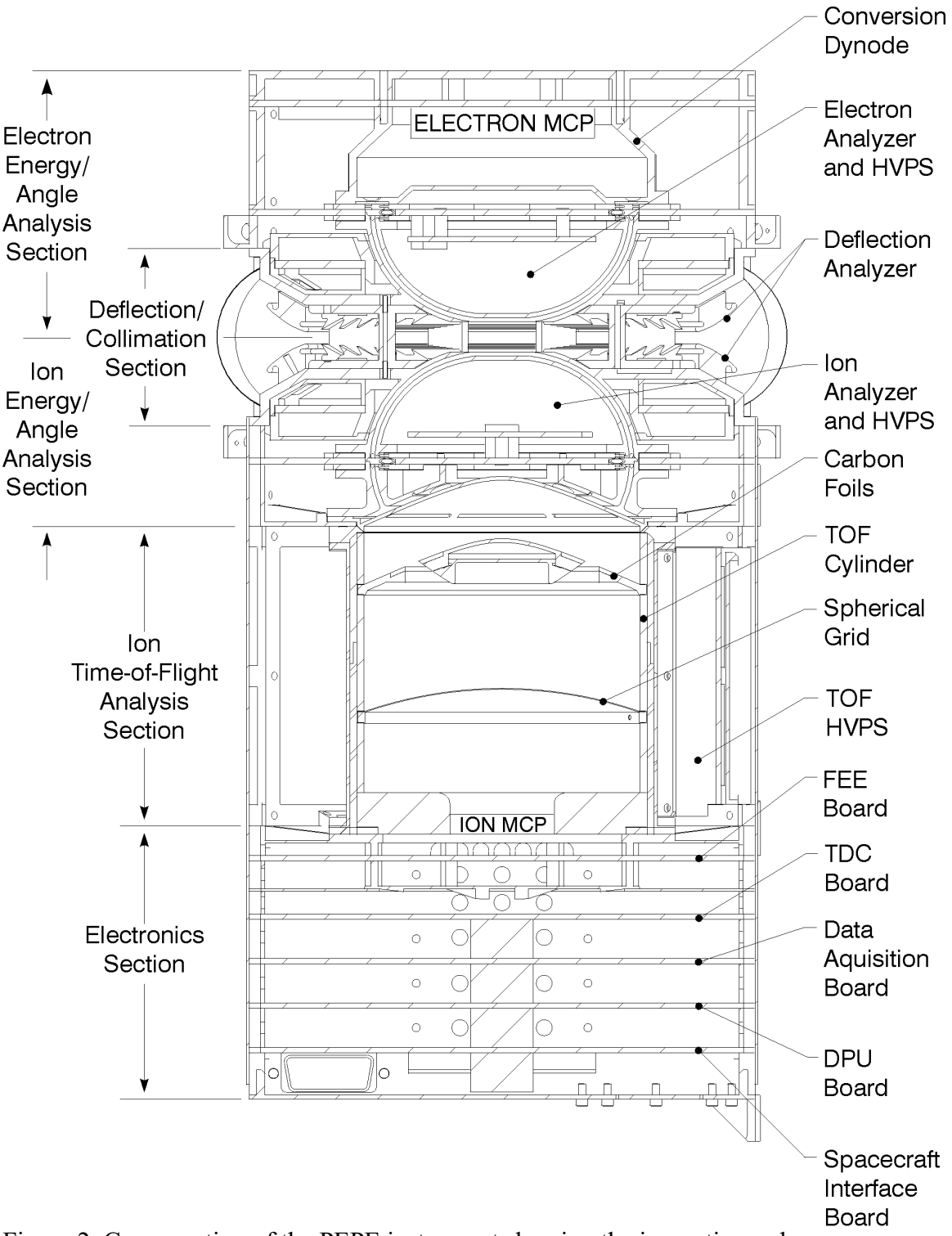

Figure 2. Cross-section of the PEPE instrument showing the ion optics and electronics.

Figure 3. Photograph showing PEPE mounted on the DS1 spacecraft.

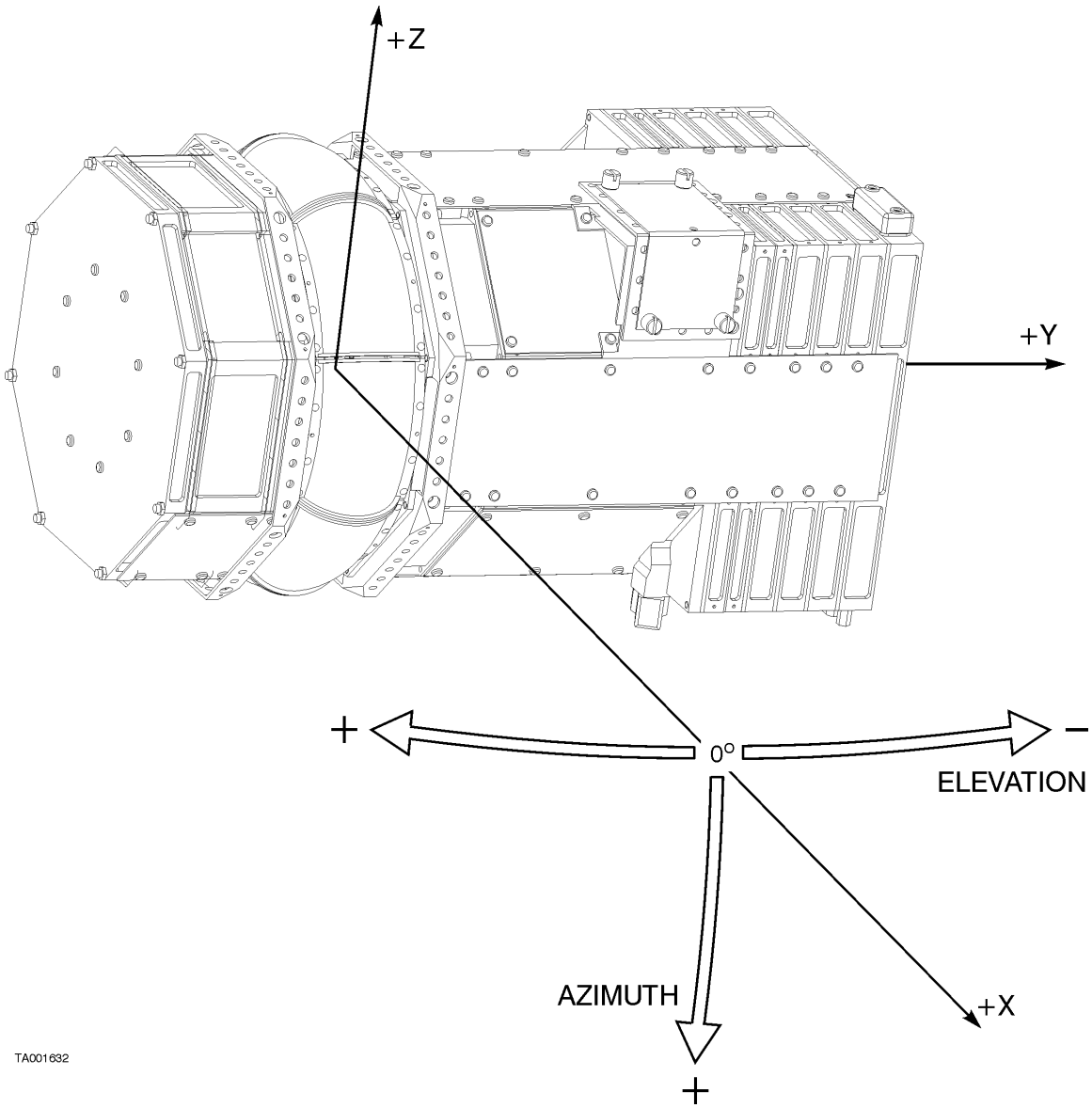

Figure 4. Diagram showing the PEPE elevation and azimuth directions.

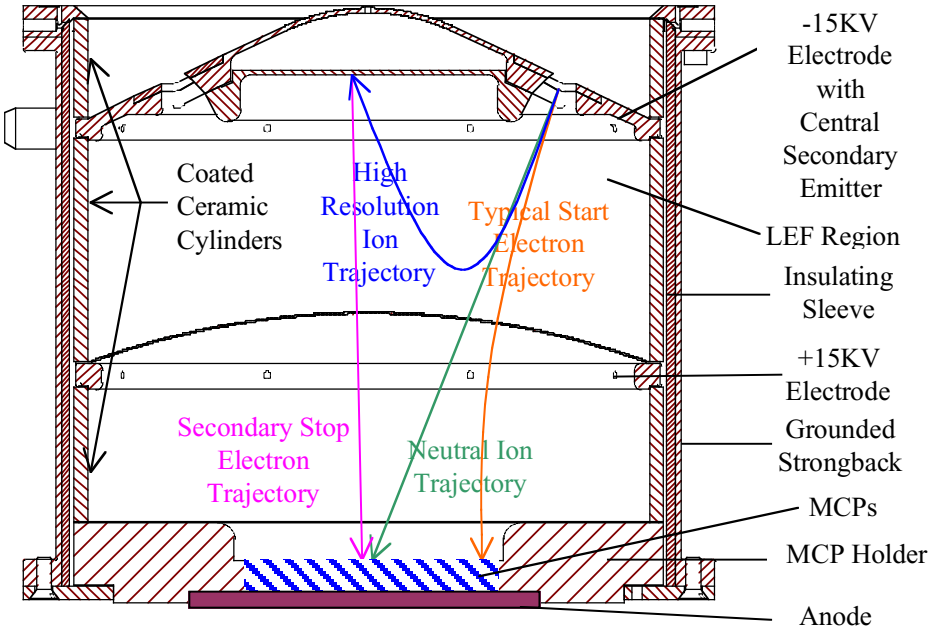

Figure 5. Cross-section schematic of the PEPE TOF cylinder.

Figure 6. Photograph showing the TOF analyzer MCP holder.

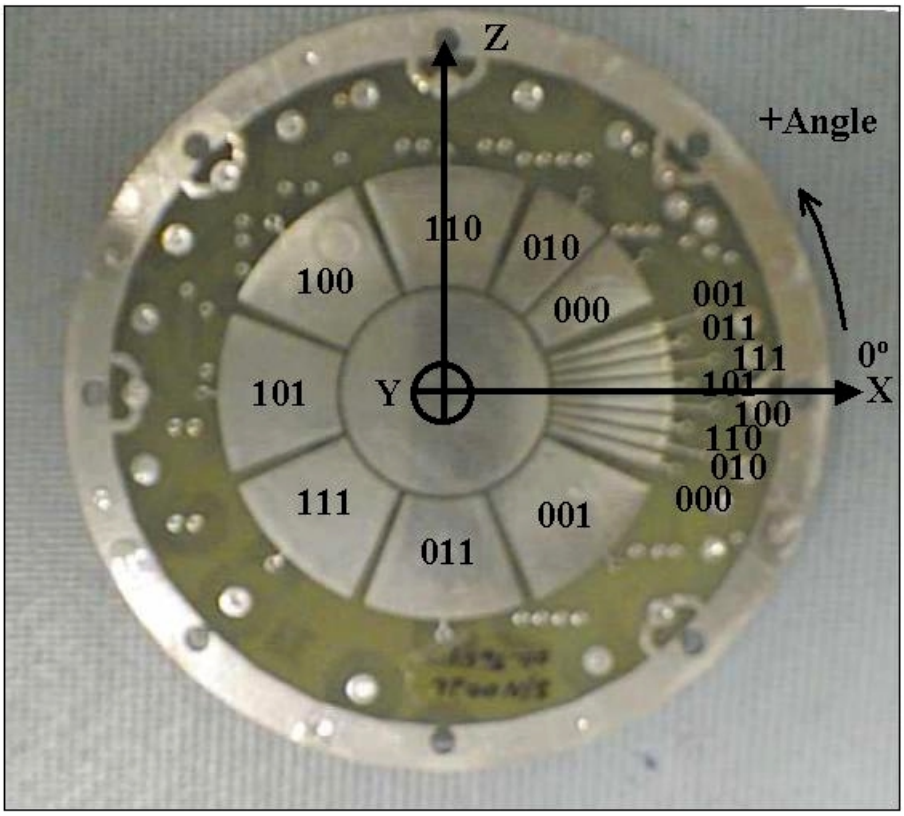

Figure 7. Photograph of the ion TOF MCP anode displaying the anode sections and numbering system.

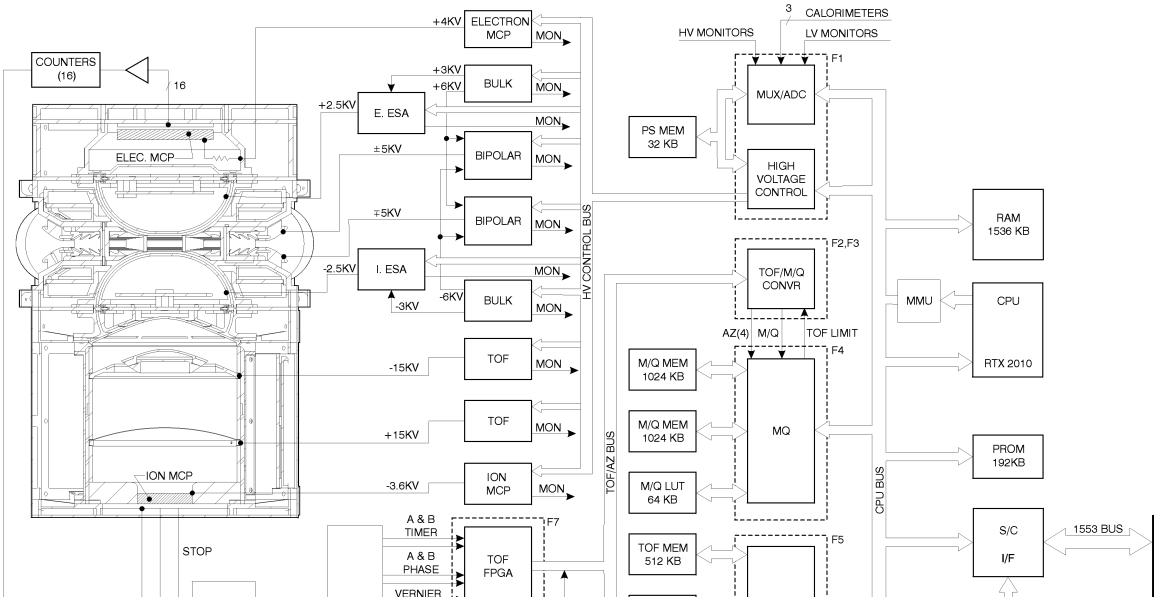
COUNTERS
(16)
16
ELEC. MCP
ION MCP
STOP
+4KV
ELECTRON
MCP
MON
+3KV
+6KV
BULK
+2.5KV
E. ESA
±5KV
BIPOLAR
∓5KV
BIPOLAR
-2.5KV
I. ESA
-6KV
-3KV
BULK
-15KV
TOF
+15KV
TOF
-3.6KV
ION
MCP
A & B
TIMER
A & B
PHASE
VERNIER
F7
TOF
FPGA
HV CONTROL BUS
TOF/AZ BUS
3
CALORIMETERS
HV MONITORS
LV MONITORS
F1
MUX/ADC
PS MEM
32 KB
HIGH
VOLTAGE
CONTROL
F2,F3
TOF/M/Q
CONVR
AZ(4)
M/Q
TOF LIMIT
F4
MQ
M/Q MEM
1024 KB
M/Q MEM
1024 KB
M/Q LUT
64 KB
TOF MEM
512 KB
F5
CPU BUS
RAM
1536 KB
MMU
CPU
RTX 2010
PROM
192KB
S/C
I/F
1553 BUS

DRAFT